

Electronic Supplementary Information

for

Inhibition and recovery of anaerobic granular sludge performances in response to short-term polystyrene nanoparticles exposure

Yue Feng^a, Li-Juan Feng^a, Shu-Chang Liu^b, Jian-Lu Duan^a, Yi-Bing Zhang^a, Shi-Chang Li^a, Xiao-Dong Sun^a, Shu-Guang Wang^a, Xian-Zheng Yuan^{a*}

^a Shandong Key Laboratory of Water Pollution Control and Resource Reuse, School of Environmental Science and Engineering, Shandong University, Qingdao, Shandong Province 266237, P. R. China

^b College of Science and Engineering, Yantai Academy of China Agricultural University, Yantai, Shandong Province 264670, P. R. China

Corresponding authors:

Xian-Zheng Yuan

School of Environmental Science and Engineering, Shandong University

72 Rd. Binhai, Qingdao, Shandong Province 266237, P. R. China

Tel./Fax: +86-532-5863 0968

E-mail: xzyuan@sdu.edu.cn (Yuan X.)

This electronic supplementary information contains 4 tables and 4 figures.

1. Synthesis of polystyrene nanoparticles (PS-NPs)

Functionalized PS-NPs (PS-SO₃H and PS-NH₂) were synthesized in our laboratory through the miniemulsion polymerization method. The styrene monomer was washed three times by a base solution (10% NaOH) to remove its inhibitor. The anionic PS-SO₃H was synthesized with sodium dodecyl sulfate (SDS) as emulsifiers and potassium persulphate (KPS) as initiator.^{1, 2} The cationic PS-NH₂ was synthesized through nitrogen-protected polymerization for 5 h at 80 °C with the stirring rate fixed at 400 rpm with dodecylamine hydrochloride and 2, 2'-azobisisobutyronitrile (AIBN). After the synthesis, the latex was transferred to dialysis bag (1 kDa) for removing styrene monomer, emulsifier, initiator and other impurities in the reaction system. The diameter and morphologies of PS-NPs were characterized by a scanning electron microscope (Hitachi S-5000, Hitachi, Japan). Size (Z-average) and ζ-potential (mV) were determined using dynamic light scattering (Zetasizer Nano ZS, Malvern, UK). The number and size/concentration of particles were measured by a NanoSight NS500 (NanoSight, Amesbury, UK).

2. Modified Gompertz fitting

The modified Gompertz model was used to simulate methane production. Equation 1 shows modified Gompertz equation.³ And the model simulate results are shown in Table S3.

$$Y(t) = A \exp\left(-\exp\left(\frac{\mu e}{A}(\lambda - t) + 1\right)\right) \quad \text{Equation 1}$$

Where:

Y—Cumulative of specific methane production (mL)

A—Methane production potential (mL)

μ —Maximum methane production rate (mL/h)

λ —Lag phase period (h)

t—Cumulative time for methane production (h)

e—Mathematical constant (2.718282)

3. EPS extraction

The EPS matrix was extracted using cation exchange resin method to elucidate the possible roles of EPS wrapping the AGS in response to PS-NPs.⁴ Specifically, the sludge was centrifuged at 6000 r/min for 15 min at 4 °C to remove any EPS from the bulk water. Then, the sludge pellets were resuspended to their original volume in 1% sodium chloride solution containing cation exchange resin (CER) (60 g/g MLSS). The suspension was stirred at 500 r/min for 12 h at 4 °C. The extracted EPS were collected by centrifugation of the CER and sludge mixture at 10,000 r/min for 10 min to remove the CER. Finally, the supernatants were filtered through 0.22 µm acetate cellulose membranes and lyophilized to obtain crude EPS.

4. FTIR analysis

The extracted EPS and PS-NPs were dissolved with 0.2 M phosphate buffer solution (PBS, pH 7.4) in 50 mL centrifuge tubes. Then, the mixed solution was put into an oscillator to mix and balanced without stirring for 6 h at 37 °C before spectral analysis. The infrared spectra of EPS with or without PS-NPs were measured in potassium bromide pellets using an FTIR spectrometer (Aratar, Thermo NicoLet, USA) at wavenumbers from 4000 to 400 cm^{-1} . Each spectrum was collected with a resolution of 2 cm^{-1} , and the ordinate was expressed as absorbance. To obtain detailed information regarding protein secondary structures, the amide I region (1700–1600 cm^{-1}) of the FTIR spectrum was further analyzed. The amide I region was deconvoluted to divided overlapping peaks by increasing the spectral resolution. Then, the spectrum was further broken up into component peaks as protein secondary structures through nine-point Savitzky-Golay derivative function analysis and smoothing.⁵ A Lorentzian line shape was quantitated for the amide I region prior to curve fitting the original spectra using Peakfit 4.12 software.

Table S1 The compositions of synthetic wastewater

Components	Elements	Concentration (g/L)
Constant elements	glucose	2.00
	NH ₄ Cl	0.20
	KH ₂ PO ₄	0.05
Trace elements Stock solution (Take 13.5 mL to 1 L when using)	CaCl ₂ ·2H ₂ O	16.70
	MgCl ₂ ·6H ₂ O	120.00
	KCl	86.70
	MnCl ₂ ·4H ₂ O	1.33
	CoCl ₂ ·6H ₂ O	2.00
	H ₃ BO ₃	0.38
	CuCl ₂ ·2H ₂ O	0.18
	Na ₂ MoO ₄ ·2H ₂ O	0.17
	ZnCl ₂	0.14
	FeCl ₂ ·4H ₂ O	24.67
Buffer solution	NaHCO ₃	2.00

Table S2 Primers used for qPCR amplifications in this study.

Name	Primer				
	Sequence of the primer	Target gene	Expected amplicon	Annealing (°C)	Reference
K90	GCGGTGGAGCATGTGGTTTA	16S rRNA	181bp	55	6
K94	GATAAGGGTTGCGCTCGTTG				
<i>mcrA-F</i>	TGTAACGACGGCCAGTGGTGGTGMGGATTC	<i>mcrA</i>	464bp	51	7
	ACACARTAYGCWACAGC				
<i>mcrA-R</i>	CAGGAAACAGCTATGACCTTCATTGCRTAGTTW				
	GGRTAGTT				
<i>ACAS-F</i>	TAATCCGCCAAAAGAGTTGG	<i>ACAS</i>	138bp	56	8
<i>ACAS-R</i>	TCTTCTGGACTGGCTGGTCT				

Table S3 Modified Gompertz parameters.

Sample	First cycle				Second cycle			
	A (mL)	λ (h)	μ (mL/h)	R ²	A (mL)	λ (h)	μ (mL/h)	R ²
blank	51.29	9.11	0.39	0.99	9.75	2.33	0.21	0.98
60 μ g/mL PS-SO ₃ H	52.10	8.88	0.39	0.98	9.40	6.51	0.28	0.99
80 μ g/mL PS-SO ₃ H	50.88	1.48	0.44	0.98	10.94	9.57	0.34	0.99
100 μ g/mL PS-SO ₃ H	42.81	-1.32	0.30	0.97	11.39	8.53	0.27	0.99
5 μ g/mL PS-NH ₂	49.84	4.41	0.38	0.99	11.41	11.20	0.27	0.99
10 μ g/mL PS-NH ₂	45.87	6.55	0.39	0.98	8.45	8.73	0.23	0.99
20 μ g/mL PS-NH ₂	40.17	5.37	0.41	0.99	10.26	6.12	0.25	0.99

Table S4. The relative abundances of Archaea phyla in the first and second cycles.

tax_name	First cycle			Second cycle		
	Blank	100 µg/mL	20 µg/mL	Blank	100 µg/mL	20 µg/mL
		PS-SO ₃ H	PS-NH ₂		PS-SO ₃ H	PS-NH ₂
Euryarchaeota	99.61	99.81	99.52	99.60	99.43	99.48
Pacearchaeota	0.22	0.05	0.39	0.09	0.05	0.09
Crenarchaeota	0.10	0.06	0.05	0.17	0.45	0.34
Woesearchaeota	0.07	0.08	0.02	0.14	0.06	0.09
Other	0.0	0.0	0.02	0.0	0.01	0.0

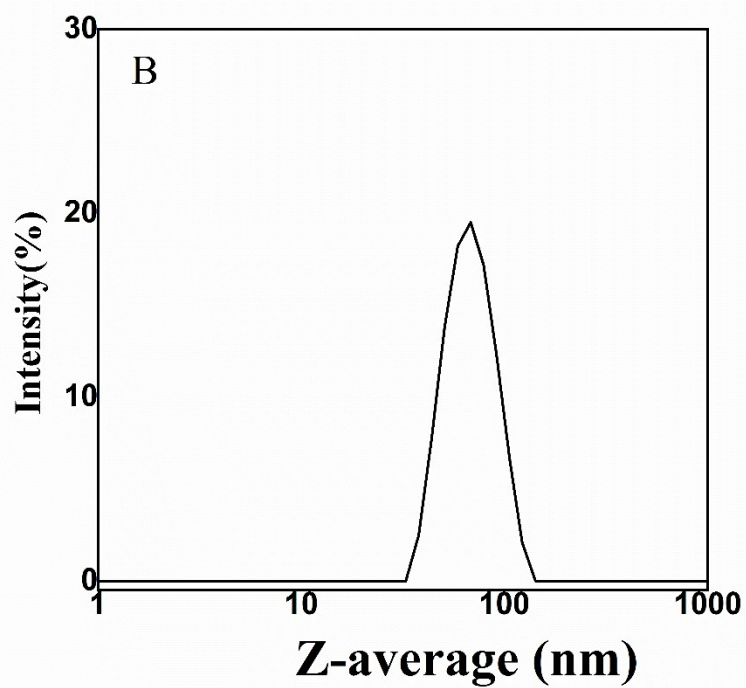
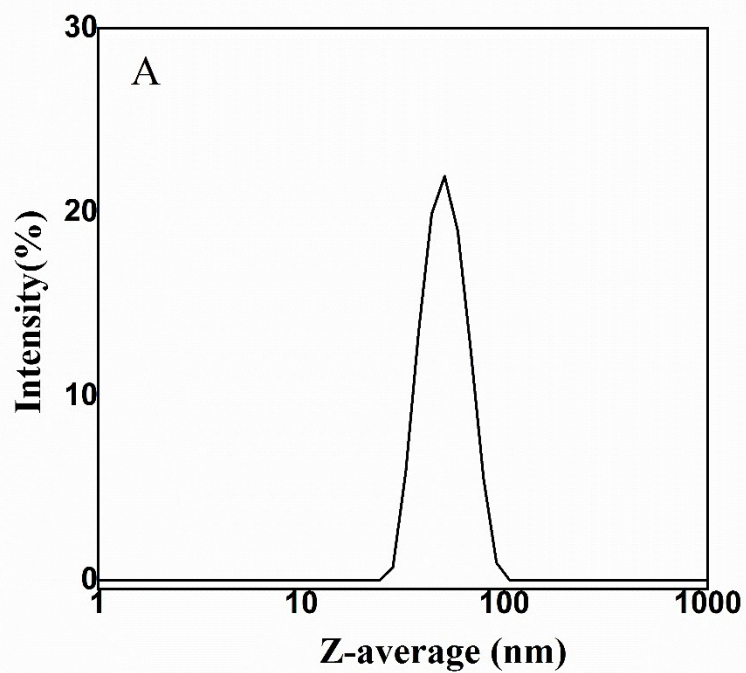
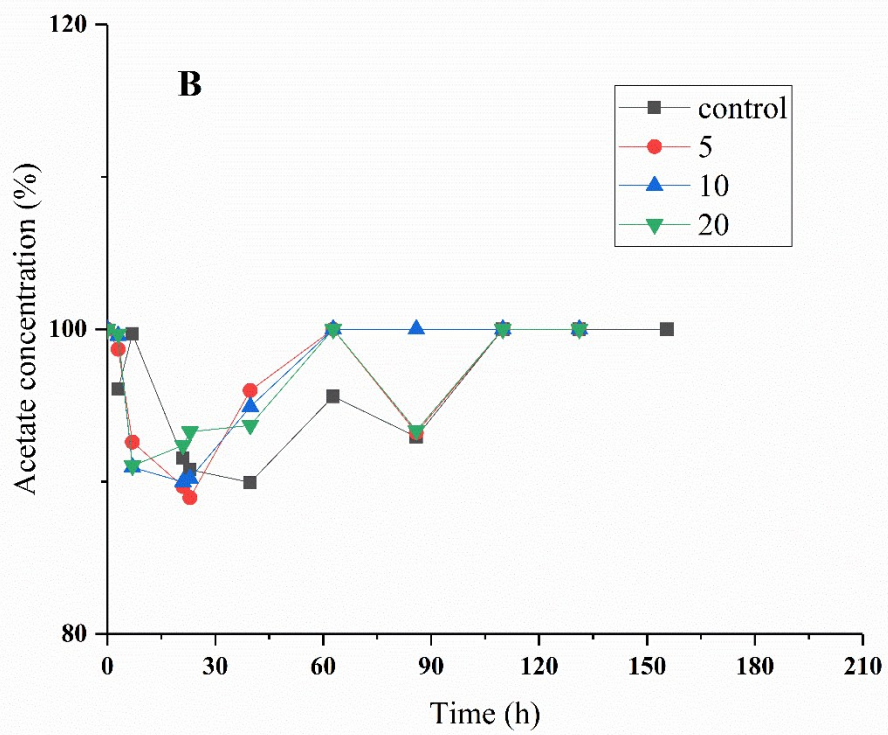
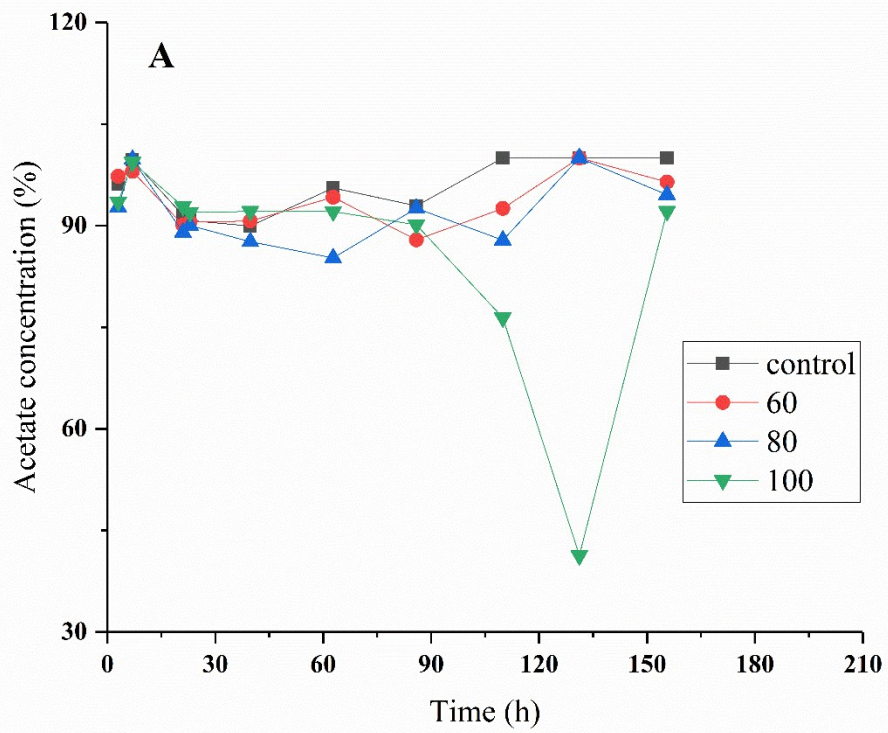


Fig. S1 The dynamic light scattering of the synthetic (A) PS-SO₃H and (B) PS-NH₂.



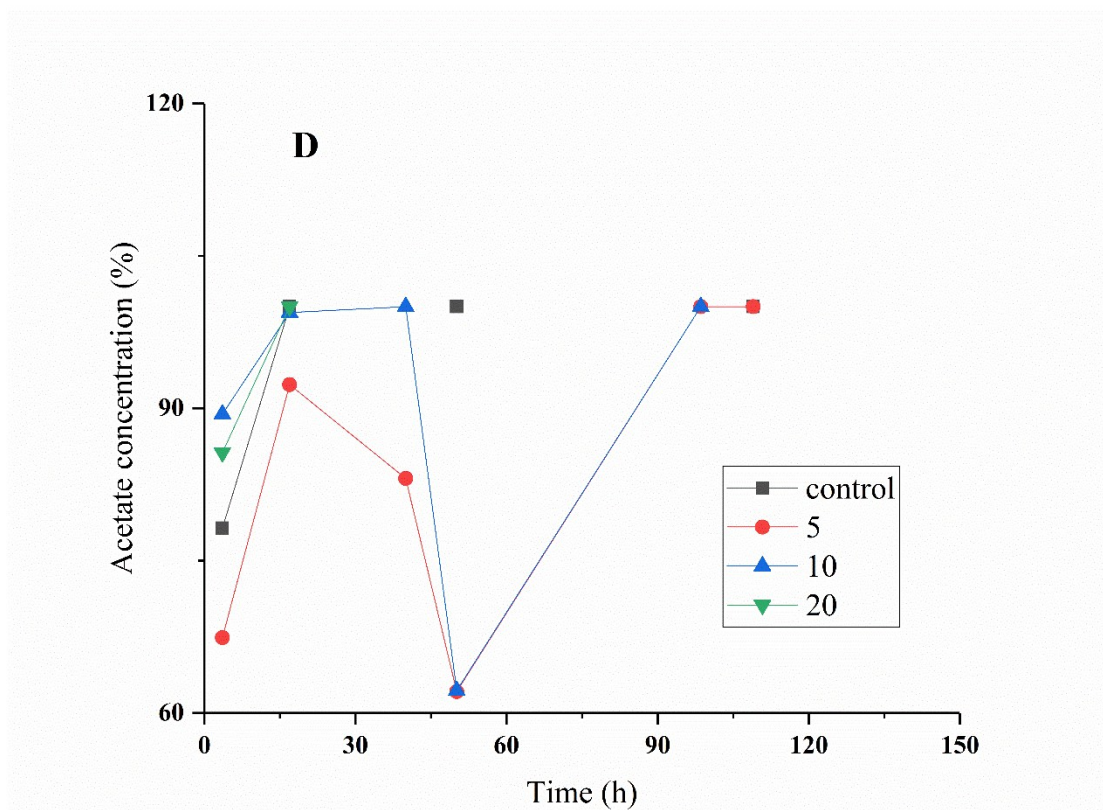
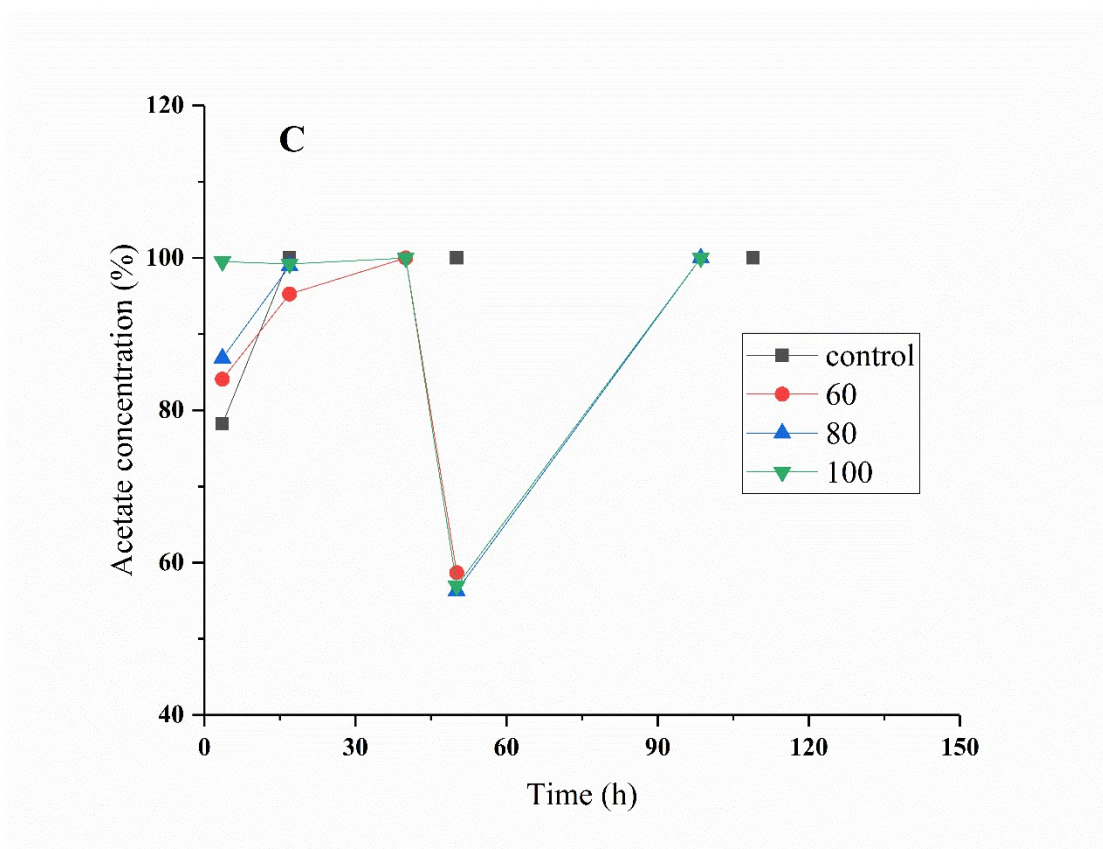


Fig. S2 The concentration of acetate in VFAs for exposure to (A) PS-SO₃H at 1st cycle, (B) PS-NH₂ at 1st cycle, (C) PS-SO₃H at 2nd cycle and (D) PS-NH₂ at 2nd cycle.

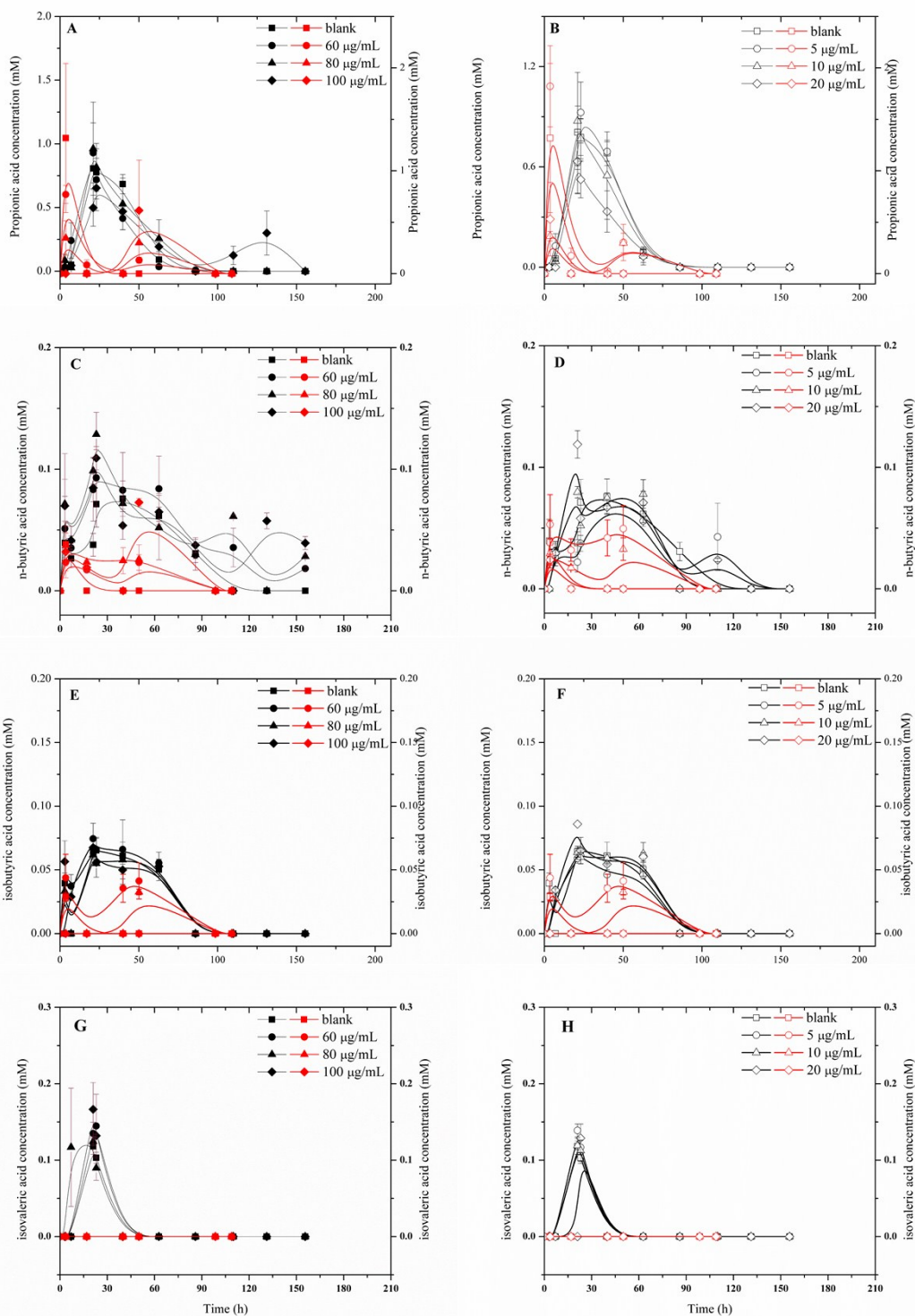


Fig. S3 Curves of other VFAs over time for the first (black) and second (red) cycle: propionic acid (A: PS-SO₃H and B: PS-NH₂); n-butyric acid (C: PS-SO₃H and D: PS-NH₂); isobutyric acid (E: PS-SO₃H and F: PS-NH₂); isovaleric acid (G: PS-SO₃H and H: PS-NH₂).

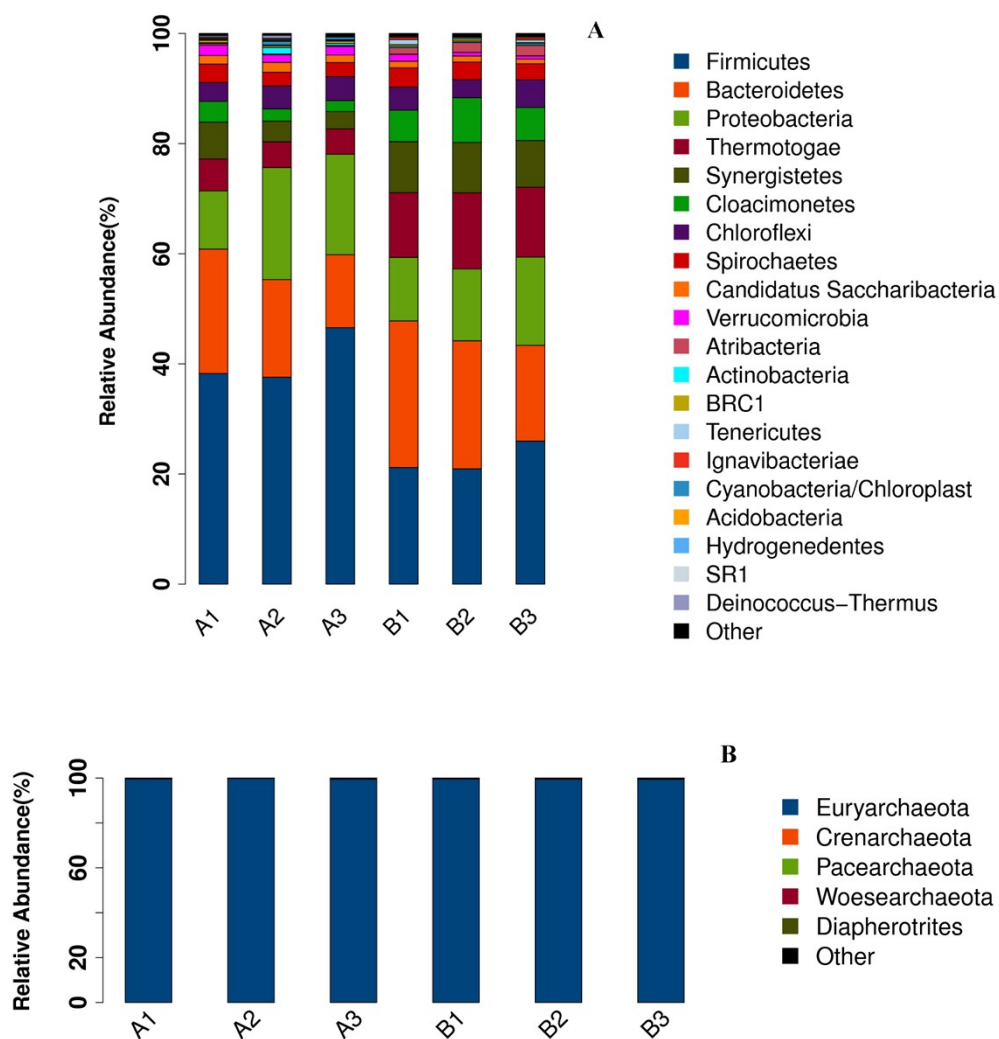


Fig. S4 The relative abundances of (A) bacterial and (B) archaeal phylum of A1: blank, A2: 100 $\mu\text{g}/\text{mL}$ PS-SO₃H and A3: 20 $\mu\text{g}/\text{mL}$ PS-NH₂ after 1st cycle; B1: blank, B1: 100 $\mu\text{g}/\text{mL}$ PS-SO₃H and B3: 20 $\mu\text{g}/\text{mL}$ PS-NH₂ after 2nd cycle.

References

1. F. Wang, G. Q. Liu, H. L. Meng, G. Guo, S. J. Luo and R. B. Guo, Improved methane hydrate formation and dissociation with nanosphere-based fixed surfactants as promoters, *ACS Sustain. Chem. Eng.*, 2016, **4**, 2107-2113.
2. J. Wang and W. Fang, A structured method for the traffic dispatcher error behavior analysis in metro accident investigation, *Safety Sci.*, 2014, **70**, 339-347.
3. W. Zhang, Q. Wei, S. Wu, D. Qi, W. Li, Z. Zuo and R. Dong, Batch anaerobic co-digestion of pig manure with dewatered sewage sludge under mesophilic conditions, *Appl. Energ.*, 2014, **128**, 175-183.
4. F. P. Zhu, J. L. Duan, X. Z. Yuan, X. S. Shi, Z. L. Han and S. G. Wang, Hydrolysis, adsorption, and biodegradation of bensulfuron methyl under methanogenic conditions, *Chemosphere*, 2018, **199**, 138-146.
5. C. Yin, F. Meng and G.-H. Chen, Spectroscopic characterization of extracellular polymeric substances from a mixed culture dominated by ammonia-oxidizing bacteria, *Water Res.*, 2015, **68**, 740-749.
6. N. Guo, Y. Wang, T. Tong and S. Wang, The fate of antibiotic resistance genes and their potential hosts during bio-electrochemical treatment of high-salinity pharmaceutical wastewater, *Water Res.*, 2018, **133**, 79-86.
7. P. E. Luton, J. M. Wayne, R. J. Sharp and P. W. Riley, The *mcrA* gene as an alternative to 16S rRNA in the phylogenetic analysis of methanogen populations in landfill b, *Microbiology*, 2002, **148**, 3521-3530.
8. B. Ince, G. Koxsel, Z. Cetecioglu, N. A. Oz, H. Coban and O. Ince, Inhibition effect of isopropanol on acetyl-CoA synthetase expression level of acetoclastic methanogen, *Methanosaeta concilii*, *J. Biotechnol.*, 2011, **156**, 95-99.